Hysteresis Current Control Schemes for Vector Controlled Induction Motor Drives

**M. Rama Prasad Reddy[1], T. Brahmananda Reddy[2],
and B. Brahmaiah[3]**

[1]*EEE Department, Sri Vasavi Engineering College, T.P. Gudem, A.P., India*
[2]*EEE Department, G. Pulla Reddy Engineering College (Autonomous),
Kurnool, A.P., India.*
[3]*Guntur Engineering College, Guntur, India*
mrpreddy77@gmail.com, tbnr@rediffmail.com

Abstract

This paper presents a simple vector control scheme for the induction motor drives. In the proposed vector control algorithm, generation of the reference currents is as per conventional vector control and voltage vector selection as per direct torque control. So the proposed vector control algorithm integrates the principles of both conventional vector control and direct torque control. The proposed lookup tables based vector control gives good dynamic response with reduced harmonic distortion. In this paper a 6-sector and 12-sector based vector control algorithm is presented. To validate the proposed methods numerical simulation studies are carried out and compared with the existing algorithms. The simulation results show the effectiveness of the proposed algorithm.

Keywords— DTC, Induction motor, switching table, vector control

Introduction

The induction motors are used in many industrial applications because of less maintenance and low weight volume ratio. In such applications speed control of induction motors are also important. Many schemes have been proposed for the speed control of induction motor drives in the literature. Among which scalar control (V/f) of induction motor proposed in [1] has the advantages of constant maximum torque but has sluggish response due to coupling between torque and flux. To overcome this drawback, the field oriented control (FOC), which is also known as vector control is developed in [2, 4-6]. By using the FOC, the torque and flux of induction motor can

be controlled independently as in separately excited DC motors. This control algorithm gives high starting torque and gives fast response due to decoupled control. Though vector control method gives decoupled control, it requires reference frame transformations, which increases the complexity of system.

To reduce the complexity of vector control algorithm in 1980s, Takahashi proposed direct torque control (DTC) technique for induction motor drives [3]. The DTC algorithm do not need coordinate transformation and PWM modulator when compared with vector control strategy. DTC is simple to implementation, because it needs only two hysteresis comparators and a switching table to control both the flux and torque. But, the DTC gives large steady state ripples in torque, flux and current. The comparative study of FOC and DTC has presented in [7].To reduce the complexity involved in the current controlled induction motor drives, a lookup table based approach has presented in [8]. This gives the good performance with reduced complexity.

To overcome the drawbacks of conventional vector control and direct torque control algorithms, in this paper novel vector control scheme, which combines the principles of both vector control and DTC is proposed. To reduce the torque ripple and to maintain a constant switching frequency, a simple 6 sector based algorithm is introduced. A 12 sector algorithm is also proposed for further reduction in THD. The proposed algorithm uses sophisticated lookup tables to generate the PWM signals to the inverter. Moreover, the proposed methods do not require reference frame transformations and gives good steady state and transient performance.

Conventional Vector Control Method

The conventional vector control technique gives a decoupled torque and flux control like a separately excited dc motor and gives fast torque response. To achieve decoupled control stator current vector is resolved into two components, torque producing component (i_{qs}^*) and flux producing component (i_{ds}^*). These components are represented in synchronous reference frame so as to appear in DC quantities.

The electromagnetic torque of an induction motor is given as

$$T_e = \frac{3}{2}\frac{P}{2}\frac{L_m}{L_r}\left(\psi_{dr}i_{qs} - \psi_{qr}i_{ds}\right) \tag{1}$$

In FOC, the i_{ds}^* is oriented along the rotor flux linkage vector, and the i_{qs}^* is perpendicular to it. Thus, the entire rotor flux is aligned along d-axis and hence the q-axis flux component will become zero. Hence, the torque expression can be modified as given in (2).

$$T_e = \frac{3}{2}\frac{P}{2}\frac{L_m}{L_r}\left(\psi_{dr}i_{qs}\right) \tag{2}$$

Hence, the total rotor flux can be given as in (3).

$$\psi_r = \psi_{dr} = L_m i_{ds} \tag{3}$$

From (3), it can be observed that the rotor flux is directly proportional to i_{ds}^* and is maintained constant. Hence, the torque depends on i_{qs}^*, and provides a torque response as fast as the i_{qs}^* response and hence decoupled control between torque and flux is achieved. In order to transform these DC quantities or synchronous reference frame quantities to stationary reference frame, angle (θs) should be known. This estimation of angle divides the FOC in to direct vector control and indirect vector control. In indirect vector control this angle is estimated as shown by equation (4). The slip speed can be estimated by using equation (5).

$$\theta_s = \theta_r + \theta_{sl} = \int (\omega_r + \omega_{sl})dt = \int \omega_s dt \tag{4}$$

$$\omega_{sl} = \frac{L_m R_r}{L_r \lambda_r} i_{qs}^* \tag{5}$$

Proposed Vector Control Algorithms

The electromagnetic torque of an induction motor can also be represented as

$$T_e = \frac{3}{2} \frac{P}{2} \frac{L_m}{L_r} |\bar{\lambda}_r| |\bar{i}_s| \sin \delta \tag{6}$$

where δ is the angle between stator current and rotor flux linkage vectors as shown in Fig. 1. From (6), it can be concluded that the torque can be controlled by varying the δ. This is the basic principle of proposed vector control algorithm. For a short time interval, the rotor flux linkage vector is almost unchanged in space. Hence, the rapid changes of electromagnetic torque can be produced by rotating the stator current vector in the required direction according to the reference torque.
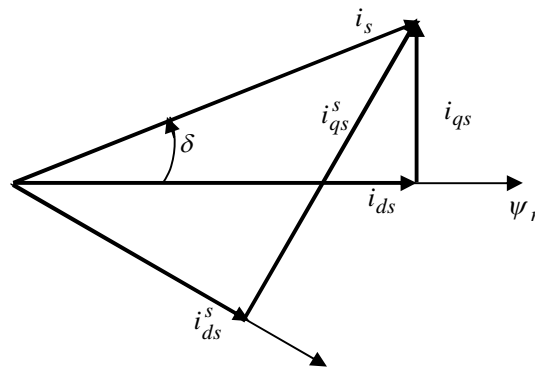
Fig. 1 Representation of stator current and rotor flux linkage space vectors

The simplified stator voltage of an induction motor can be expressed as (by ignoring the stator resistance drop)

$$\bar{v}_s = \frac{d\bar{\psi}_s}{dt} \tag{7}$$

The stator and rotor flux linkage vectors of an induction motor can be given as

$$\overline{\psi}_s = L_s \overline{i}_s + L_m \overline{i}_r \tag{8}$$

$$\overline{\psi}_r = L_r \overline{i}_r + L_m \overline{i}_s \tag{9}$$

From (9), the expression for rotor current can be obtained as

$$\overline{i}_r = \frac{\overline{\psi}_r - L_m \overline{i}_s}{L_r} \tag{10}$$

By substituting (10) in (8), the stator flux linkage expression can be obtained as given in (11).

$$\overline{\psi}_s = L_s \overline{i}_s + \frac{L_m}{L_r} \psi_r - \frac{L_m^2}{L_r} \overline{i}_s \tag{11}$$

For short time durations, by assuming the rotor flux linkage vector as constant, the voltage expression can be simplified as follows.

$$\overline{v}_s = \frac{d\overline{\psi}_s}{dt} = \left(L_s - \frac{L_m^2}{L_r} \right) \frac{d\overline{i}_s}{dt} = \sigma L_s \frac{d\overline{i}_s}{dt} \tag{12}$$

where σ is the leakage coefficient of induction motor. From (12), for a short time interval of Δt, the stator current can be given as

$$\Delta \overline{i}_s = \frac{1}{\sigma L_s} \overline{v}_s \Delta t \tag{13}$$

Thus, the stator current vector moves in the direction of the stator voltage space vector at a speed proportional to magnitude of voltage space vector. By selecting a proper voltage vector it is then possible to change the stator current in the required direction. The decoupled control of the torque and flux can be achieved by controlling the $\overline{i}_{ds}$ and $\overline{i}_{qs}$ components of the stator current. Assume, a slow motion for $\overline{\lambda}_r$, if an active voltage vector is applied then it causes rapid movement of $\overline{i}_s$ and torque increases. On the other hand, when a zero voltage vector is used, $\overline{i}_s$ becomes stationary and the electromagnetic torque will decrease, since rotor flux continues to move in the forward direction slowly and the angle δ decreases. Thus, the variation of current vector can be controlled by using the different voltage vectors in each sampling time period as shown in Fig. 2.

Fig. 2 movement of stator current vector under the influence of voltage vectors

The block diagram for the proposed FOC is shown in Fig. 3. In the proposed FOC algorithm generates the reference stator current components, which are at synchronously rotating reference frame. Then it uses hysteresis controllers and a lookup table. Thus, the proposed algorithm eliminates time consuming PWM procedure and reference frame transformations. The reference currents are compared with their actual current values, which are obtained from the measured phase currents. These current errors are used to as inputs to the hysteresis controllers. Based on the outputs of hysteresis controllers and position of the stator current vector, the lookup table will give the suitable voltage vector.

Fig. 3 Block diagram of proposed vector controlled induction motor drive

Six Sector Based Vector Control
The operating states of three phase voltage source inverter can be divided in to active and zero states. There are six active states and two zero states these states can be represented graphically as shown in Fig.4

$\overline{V}_3 (010)$ $\overline{V}_2 (110)$

Sector I

$\overline{V}_4 (011)$ $\overline{V}_1 (100)$

$\overline{V}_0 (000)$

$\overline{V}_7 (111)$

$\overline{V}_5 (001)$ $\overline{V}_6 (101)$

Fig. 4 Possible voltage space vectors for VSI

Based on the position of stator current vector, it is possible to switch the suitable voltage vectors to control both $\bar{i}_{ds}$ and $\bar{i}_{qs}$. The space plane is divided into six symmetrical sectors. As six sectors are symmetrical, here the discussion is limited to first sector only. If at any instant of time the stator current vector is in sector I as shown in Fig. 5, then voltage vectors $\overline{V}_2$ and $\overline{V}_6$ can increase the flux component current $\bar{i}_{ds}$ and $\overline{V}_3$ and $\overline{V}_5$ can decrease the $\bar{i}_{ds}$. Similarly $\overline{V}_2$ and $\overline{V}_3$ can increase the torque component current $\bar{i}_{qs}$ and $\overline{V}_5$ and $\overline{V}_6$ can decrease the $\bar{i}_{qs}$. Similarly the suitable voltage vectors can be selected for other sectors.

$\overline{V}_3 (FDTI)$ $\overline{V}_2 (FI,TI)$

ω_r

i_s

Sector 1

$\overline{V}_5 (FD,TD)$ $\overline{V}_6 (FI,TD)$
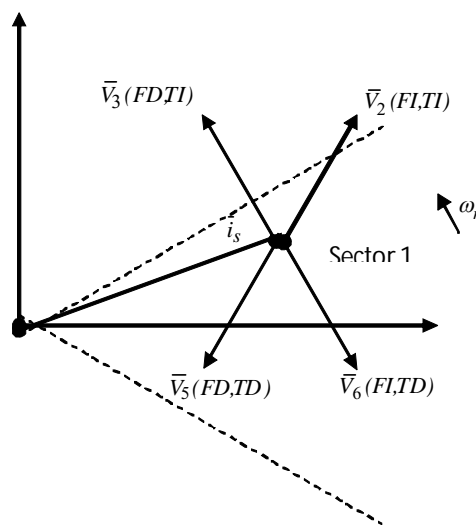
Fig. 5 selection of suitable voltage space vector in sector I (-30^0 to 30^0)

a   In the proposed FOC, the errors are restricted within their respective hysteresis bands, which are $2\Delta\bar{i}_{ds}$ and $2\Delta\bar{i}_{qs}$ wide respectively. The proposed algorithm uses hysteresis controllers which are similar to that of the controllers used in DTC. A two-level hysteresis controller to control flux component current and three-level hysteresis type controller to control torque component current. If increase in $\bar{i}_{ds}$ is required then $S_d = 1$; if decrease in $\bar{i}_{ds}$ is required then $S_d = 0$. Similarly, if increase in $\bar{i}_{qs}$ is required then $S_q = 1$, if decrease in $\bar{i}_{qs}$ is required then $S_q = -1$, and if no change in $\bar{i}_{qs}$ is required then $S_q = 0$. The digital output signals from flux component hysteresis controller (FHC) and torque component hysteresis controller (THC) can be summarized as in Table. 1.

Table. 1 digitized output values of the hysteresis controllers

Controller	Condition	Output of the controller
FHC	$\bar{i}_{ds} \leq \bar{i}_{ds}^{*} - \Delta\bar{i}_{s}$	$S_d = 1$
	$\bar{i}_{ds} \geq \bar{i}_{ds}^{*} + \Delta\bar{i}_{s}$	$S_d = 0$
THC	For anti-clockwise rotation	
	$\bar{i}_{qs}^{*} - \bar{i}_{qs} \geq \Delta\bar{i}_{qs}$	$S_q = 1$
	$\bar{i}_{qs} \geq \bar{i}_{qs}^{*}$	$S_q = 0$
	For clockwise rotation	
	$\bar{i}_{qs} \leq \bar{i}_{qs}^{*}$	$S_q = 0$
	$\bar{i}_{qs}^{*} - \bar{i}_{qs} \leq -\Delta\bar{i}_{qs}$	$S_q = -1$

Depending upon the values of S_d, S_q and the position of the stator current vector, the suitable voltage vector is applied to inverter. The lookup table of voltage vectors in different sectors is given in Table. 2.

Table. 2 Optimum voltage vector switching table

Sector S_d S_q		I	II	III	IV	V	VI
1	1	$\bar{v}_2$	$\bar{v}_3$	$\bar{v}_4$	$\bar{v}_5$	$\bar{v}_6$	$\bar{v}_1$
	0	$\bar{v}_7$	$\bar{v}_0$	$\bar{v}_7$	$\bar{v}_0$	$\bar{v}_7$	$\bar{v}_0$
	-1	$\bar{v}_6$	$\bar{v}_1$	$\bar{v}_2$	$\bar{v}_3$	$\bar{v}_4$	$\bar{v}_5$
0	1	$\bar{v}_3$	$\bar{v}_4$	$\bar{v}_5$	$\bar{v}_6$	$\bar{v}_1$	$\bar{v}_2$
	0	$\bar{v}_0$	$\bar{v}_7$	$\bar{v}_0$	$\bar{v}_7$	$\bar{v}_0$	$\bar{v}_7$
	-1	$\bar{v}_5$	$\bar{v}_6$	$\bar{v}_1$	$\bar{v}_2$	$\bar{v}_3$	$\bar{v}_4$

12- Sector Based Vector Control

In the proposed 6- sector vector control only limited active voltage vectors are used each sector. In order to utilize all six active states in each sector and to reduce the THD further, the space vector plane is divided into twelve sectors instead of six as shown in Fig. 6. However, it is necessary to define small and large variations. It is observed that V_1 will produce a large increase in flux and a small increase in torque in sector-12. On the other hand in it is observed that V_2 will produce a large increment in torque and a small increment in flux. The proposed 12-sector based vector control uses a four level torque hysteresis controller (TI: torque increase, TSI: torque small increase, TD: torque decrease and TSD: torque small decrease) and a two level flux hysteresis controller. The look-up table for 12-sector based FOC is presented in Table 3.
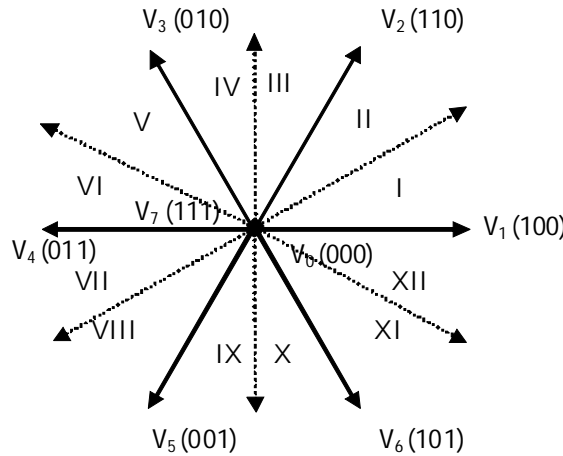
Fig. 6 Possible voltage space vectors for VSI in 12 sector based algorithm

Table. 3 Optimum voltage vector switching table

S_d	S_q	S_1	S_2	S_3	S_4	S_5	S_6	S_7	S_8	S_9	S_{10}	S_{11}	S_{12}
1	TI	$\overline{V}_2$	$\overline{V}_3$	$\overline{V}_3$	$\overline{V}_4$	$\overline{V}_4$	$\overline{V}_5$	$\overline{V}_5$	$\overline{V}_6$	$\overline{V}_6$	$\overline{V}_1$	$\overline{V}_1$	$\overline{V}_2$
	TsI	$\overline{V}_2$	$\overline{V}_2$	$\overline{V}_3$	$\overline{V}_3$	$\overline{V}_4$	$\overline{V}_4$	$\overline{V}_5$	$\overline{V}_5$	$\overline{V}_6$	$\overline{V}_6$	$\overline{V}_1$	$\overline{V}_1$
	TsD	$\overline{V}_1$	$\overline{V}_1$	$\overline{V}_2$	$\overline{V}_2$	$\overline{V}_3$	$\overline{V}_3$	$\overline{V}_4$	$\overline{V}_4$	$\overline{V}_5$	$\overline{V}_5$	$\overline{V}_6$	$\overline{V}_6$
	TD	$\overline{V}_6$	$\overline{V}_1$	$\overline{V}_1$	$\overline{V}_2$	$\overline{V}_2$	$\overline{V}_3$	$\overline{V}_3$	$\overline{V}_4$	$\overline{V}_4$	$\overline{V}_5$	$\overline{V}_5$	$\overline{V}_6$
0	TI	$\overline{V}_3$	$\overline{V}_4$	$\overline{V}_4$	$\overline{V}_5$	$\overline{V}_5$	$\overline{V}_6$	$\overline{V}_6$	$\overline{V}_1$	$\overline{V}_1$	$\overline{V}_2$	$\overline{V}_2$	$\overline{V}_3$
	TsI	$\overline{V}_4$	$\overline{V}_4$	$\overline{V}_5$	$\overline{V}_5$	$\overline{V}_6$	$\overline{V}_6$	$\overline{V}_1$	$\overline{V}_1$	$\overline{V}_2$	$\overline{V}_2$	$\overline{V}_3$	$\overline{V}_3$
	TsD	$\overline{V}_7$	$\overline{V}_5$	$\overline{V}_0$	$\overline{V}_6$	$\overline{V}_7$	$\overline{V}_1$	$\overline{V}_0$	$\overline{V}_2$	$\overline{V}_7$	$\overline{V}_3$	$\overline{V}_0$	$\overline{V}_4$
	TD	$\overline{V}_5$	$\overline{V}_6$	$\overline{V}_6$	$\overline{V}_1$	$\overline{V}_1$	$\overline{V}_2$	$\overline{V}_2$	$\overline{V}_3$	$\overline{V}_3$	$\overline{V}_4$	$\overline{V}_4$	$\overline{V}_5$

Simulation Results & Discussion

To validate the proposed vector control algorithms numerical simulation studies have been carried out in Matlab-simulink environment. For the simulation studies the motor parameters are taken as R_s =1.57Ω, R_r=1.21 Ω, L_m=0.165H, L_s=0.17H, L_r=0.17H and J=0.089 Kg-m^2. Moreover, for the simulation results equal band widths have been considered for the hysteresis bands in the proposed and existing current controlled vector controlled drives. The simulation results of classical vector controlled induction motor drive are shown in Fig.7-Fig.12. The simulation results of 6 sector based vector controlled induction motor drive are given from Fig. 13 to Fig. 18 and for proposed 12 sector based vector controlled drive are given from Fig. 19 to Fig. 24.

From the simulation results, it can be observed that the proposed algorithms give good dynamic response like conventional vector control algorithm. Also, it can be observed that the 6 - Sector algorithm gives less total harmonic distortion (THD) value when compared with the conventional vector control algorithm for same band width of the hysteresis controllers. Moreover, the 6-sector based vector control algorithm gives fixed switching frequency operation when compared with the classical vector control algorithm, which can be observed from the line voltage.

However, the conventional vector control and 6 - Sector algorithm use the zero voltage vectors. But in the proposed 12 sector based algorithm torque ripple is considerably high but the total THD in steady state is reduced. However, the proposed current controlled algorithm gives reduced THD and slight increased steady state ripples when compared with the 6 - Sector algorithm.
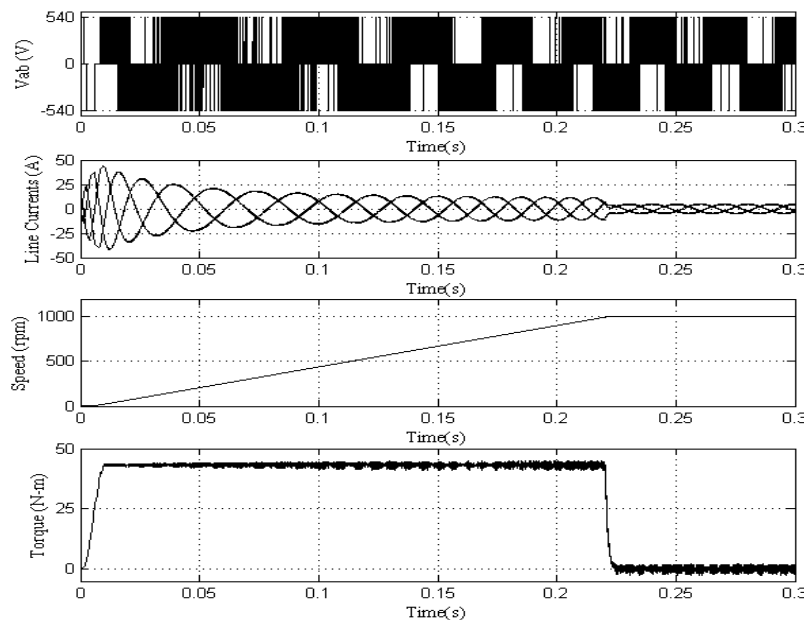
Fig. 7 starting transients of classical vector control algorithm based induction motor drive
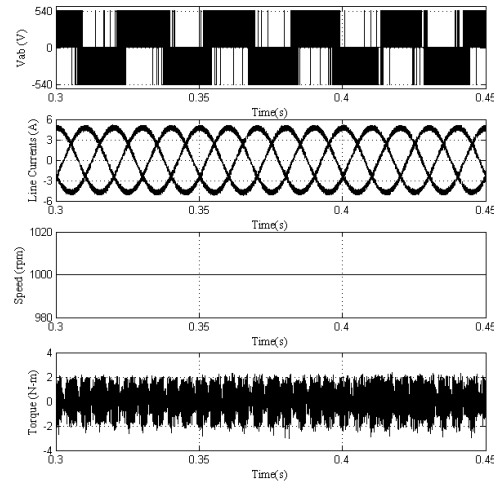
Fig. 8 steady state plots of classical vector control algorithm based induction motor drive
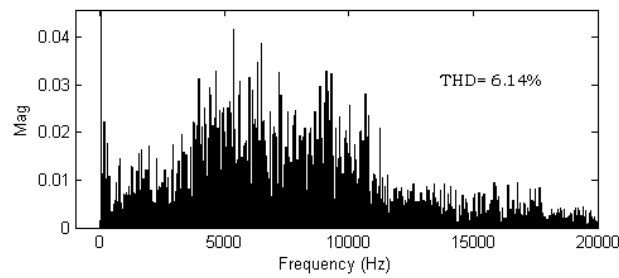
Fig. 9 Harmonic spectra of stator current in classical vector control algorithm
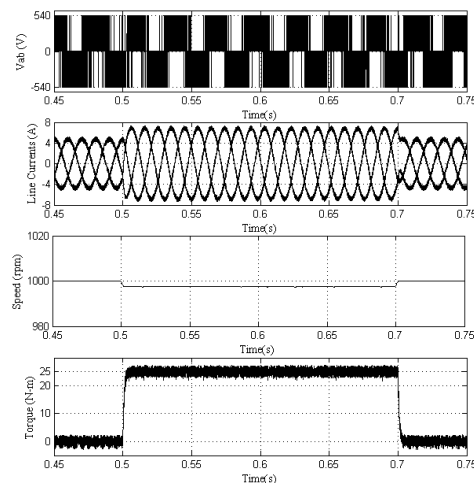
Fig. 10 Transients during the step change in load (a 25 N-m load is applied at 0.5 sec and removed at 0.7 sec) for classical vector control algorithm based induction motor drive
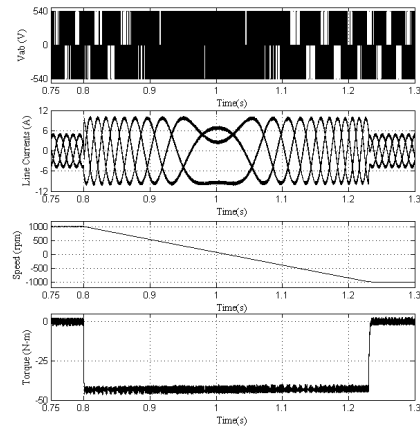
Fig. 11 Transients during the speed reversal (from +1000 rpm to -1000 rpm) for classical vector control algorithm based induction motor drive
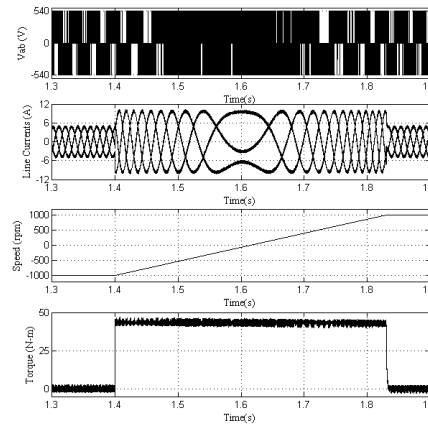
Fig. 12 Transients during the speed reversal (from -1000 rpm to +1000 rpm) for classical vector control algorithm based induction motor drive
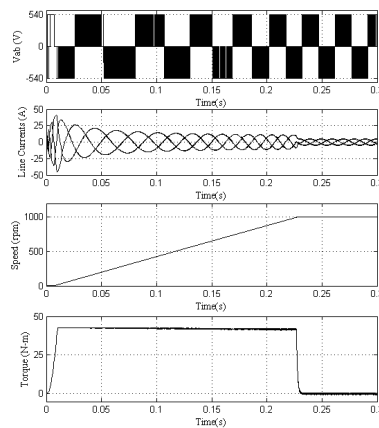
Fig. 13 starting transients of 6 - Sector algorithm vector control algorithm based induction motor drive
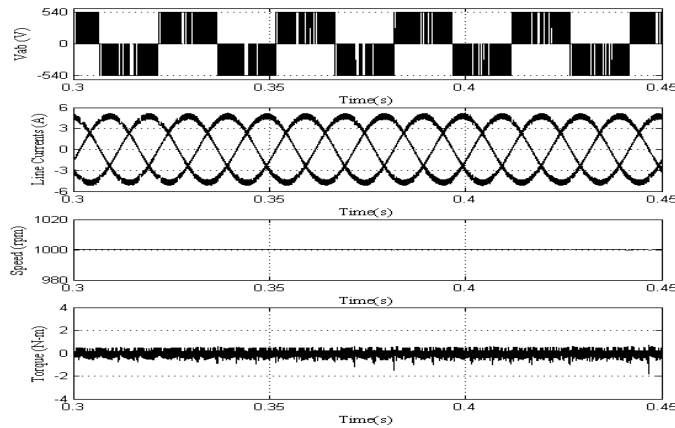
Fig. 14 steady state plots of 6 - Sector algorithm vector control algorithm based induction motor drive
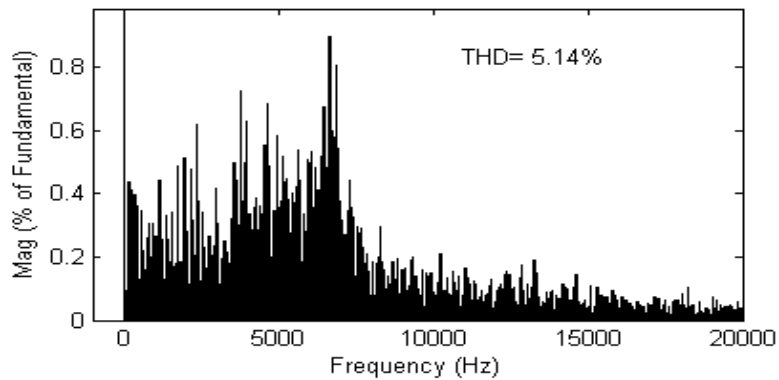
Fig. 15 Harmonic spectra of stator current in 6 - Sector algorithm vector control algorithm based induction motor drive
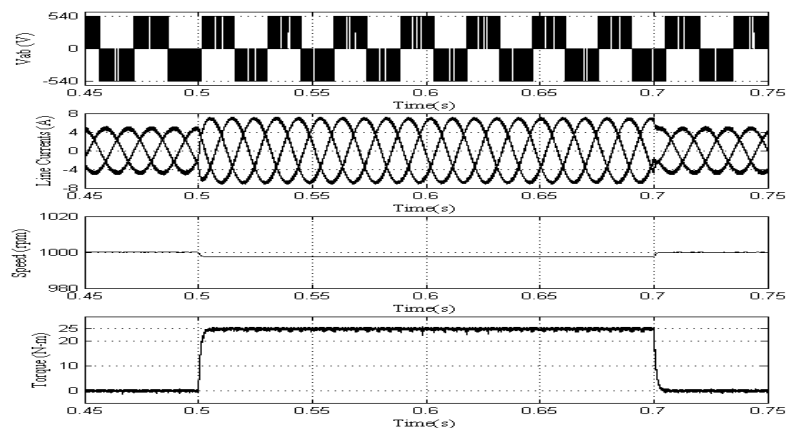
Fig. 16 Transients during the step change in load (a 25 N-m load is applied at 0.5 sec and removed at 0.7 sec) for 6 - Sector algorithm vector control algorithm based induction motor drive
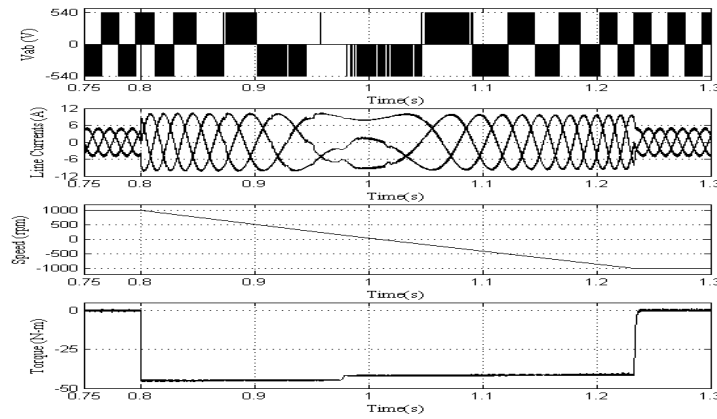
Fig. 17 Transients during the speed reversal (from +1000 rpm to -1000 rpm) for 6 - Sector algorithm vector control algorithm based induction motor drive
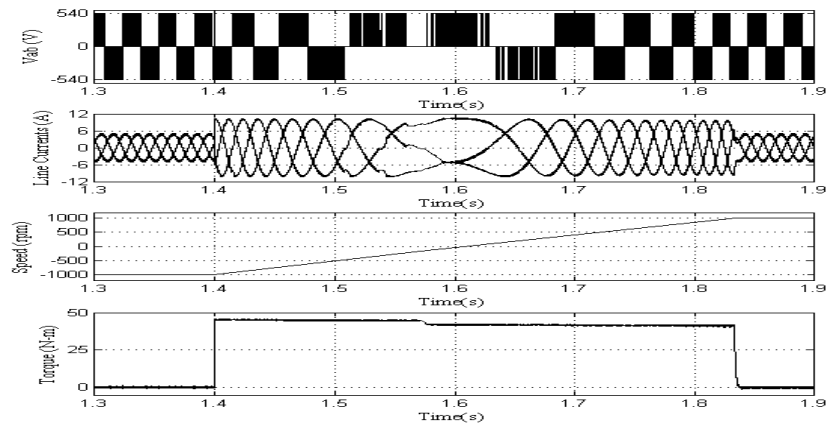
Fig. 18 Transients during the speed reversal (from -1000 rpm to +1000 rpm) for 6 - Sector algorithm vector control algorithm based induction motor drive
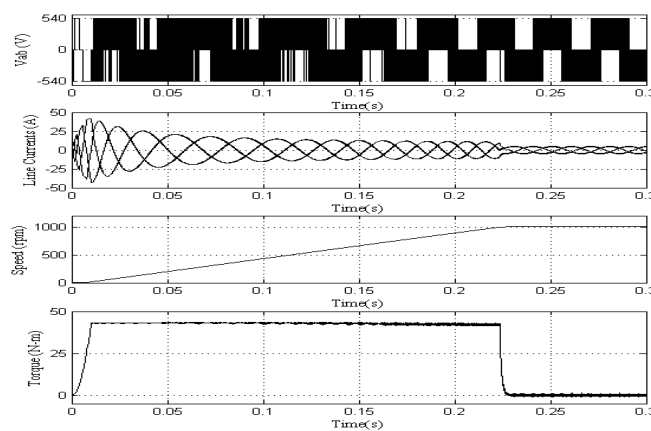
Fig. 19 starting transients of proposed 12 - Sector algorithm based vector controlled induction motor drive
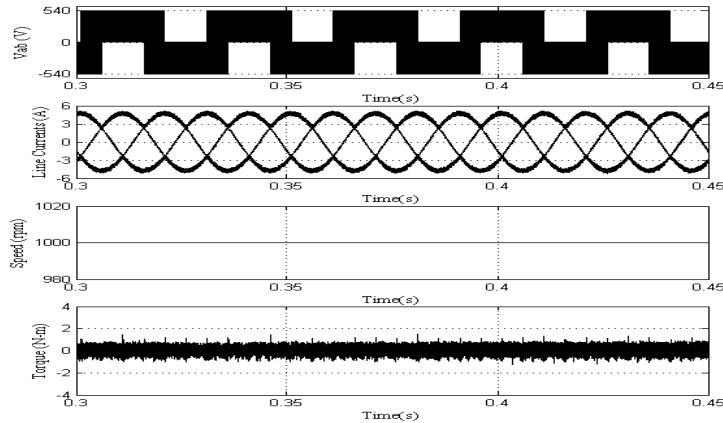
Fig. 20 steady state plots of proposed 12 - Sector algorithm based vector controlled induction motor drive
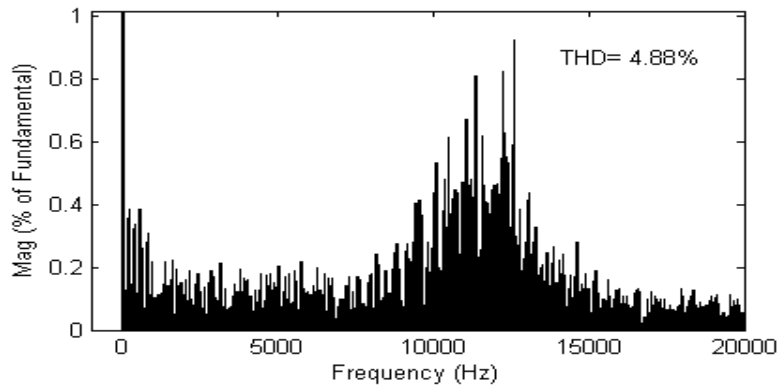
Fig. 21 Harmonic spectra of stator current in proposed 12 - Sector algorithm based vector controlled induction motor drive
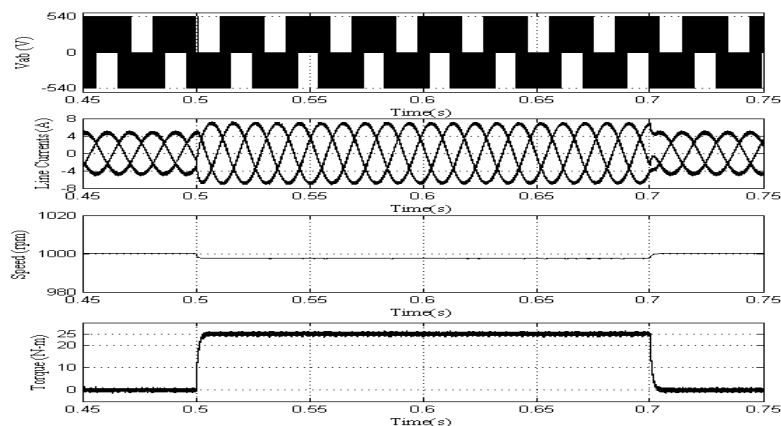
Fig. 22 Transients during the step change in load (a 25 N-m load is applied at 0.5 sec and removed at 0.7 sec) for proposed 12 - Sector algorithm based vector controlled induction motor drive
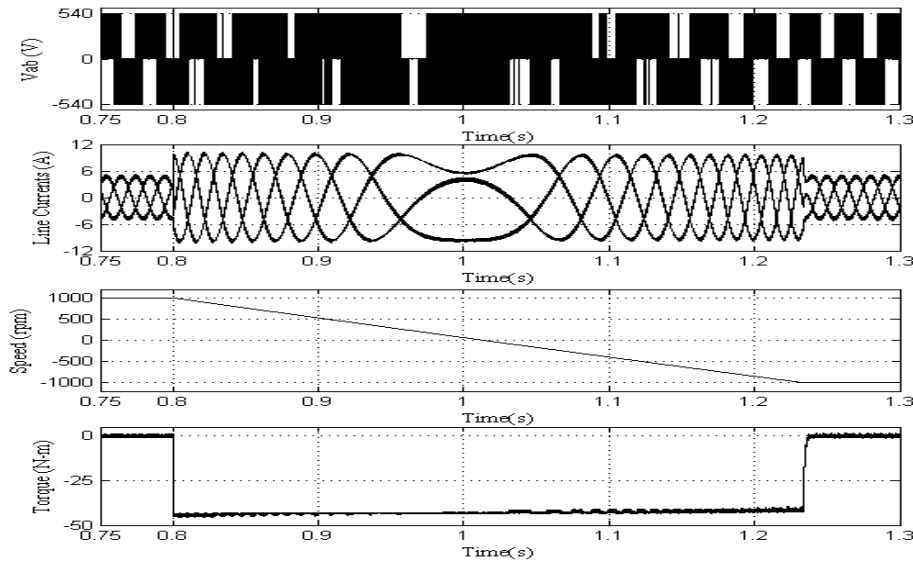
Fig. 23 Transients during the speed reversal (from +1000 rpm to -1000 rpm) for proposed 12 - Sector algorithm based vector controlled induction motor drive
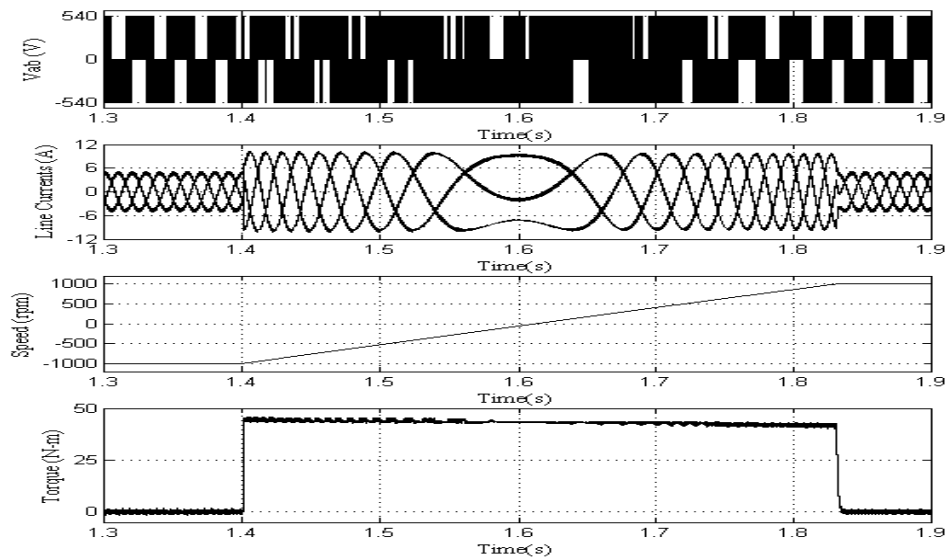
Fig. 24 Transients during the speed reversal (from -1000 rpm to +1000 rpm) for proposed 12 - Sector algorithm based vector controlled induction motor drive

Conclusions

The vector control algorithm is becoming popular in high-performance applications. Though the conventional FOC better dynamic performance, the complexity involved is more due to the reference frame transformations and PWM procedure. Hence, to reduce the complexity, a simplified FOC is presented in this paper. The proposed FOC technique uses lookup tables and eliminates the use of PWM procedure. Two

different lookup tables have been presented in this paper. The simulation results show the effectiveness of the proposed algorithms. From the results, it can be observed that the 12-sector FOC gives reduced THD when compared with the 6-sector FOC. Also, the 6-sector based vector control algorithm gives fixed switching frequency operation. Thus, the proposed algorithms reduce the complexity involved in classical FOC with good performance.

References

[1] R.Ueda and T. Sonada K Koga and M. Ichikawar "stability analysis of induction motor drives by V/f control by general purpose inverter" *IEEE Trans.Ind*.Appl .vol.28.PP 472-481.March/april 1992.

[2] F. Blaschke "The principle of field orientation as applied to the new transvector closed loop control system for rotating-field machines," *Siemens Review*, 1972, pp 217-220.

[3] Isao Takahashi, Toshihiko Noguchi, "A new quick response and high-efficiency control strategy of an induction motor", *IEEE Trans Ind Appl*, Vol.IA-22, No.5, pp. 820-827, Sep/Oct, 1986.

[4] W. Leonhard, "30 years of space vectors, 20 years of field orientation, 10 years of digital signal processing with controlled AC-drives, a review (Part1)". EPE Journal, No. 1, July 1991, pages 13-20.

[5] W. Leonhard, "30 years of space vectors, 20 years of field orientation, 10 years of digital signal processing with controlled AC-drives, a review (Part 2)". EPE Journal, No. 2, Oct, 1991, pages 89-102.

[6] J. A. Santisteban, and R. M. Stephan, "Vector control methods for induction machines: an overview," *IEEE Trans. On Education*, vol. 44, no. 2, pp. 170-175, May 2001.

[7] Domenico Casadei, Francesco Profumo, Giovanni Serra, and Angelo Tani, "FOC and DTC: Two Viable Schemes for Induction Motors Torque Control" *IEEE Trans. Power Electron.*, vol. 17, no.5, Sep, 2002, pp. 779-787.

[8] Marian P. Kaimierkowski, Maciej A. Dzieniakowski, and Waldemar Sulkowski, "Novel Space Vector Based current controllers for PWM-inverters" *IEEE Trans. Power Electronics*, vol.6, no.1, Jan, 1991, pp. 158-166.

Authors information:

M.Rama Prasad Reddy received the Bachelor of Engineering degree in Electrical & Electronics Engineering from Karnataka University of Dharwad in 1999 and Master's degree from JNTU Kakinada in 2007. He is presently pursuing Doctoral degree from JNTU, Hyderabad. Currently, working as an Associate Professor in Sri Vasavi Engineering College, Tadepalligudem, A.P. His areas of interests are in power systems, Power electronic control of drives.

Dr. T. Brahmananda Reddy was born in 1979. He graduated from Sri Krishna Devaraya University, Anantapur in the year 2001. He received M.E degree from Osmania University, Hyderabad, India in the year 2003 and Ph.D from J.N.T.University, Hyderabad in the year 2009. He is presently Professor and Head of Electrical and Electronics Engineering Department, G. Pulla Reddy Engineering College (Autonomous), Kurnool, India. He presented more than 100 research papers in various national and international conferences and journals.
His research areas include PWM techniques, DC to AC converters and control of electrical drives

Dr. B.Brahmaiah received the Bachelor of Technology degree in Electrical & Electronics Engineering from JNTU, Hyderabad in 1979, and Master's degree from National Institute of Technology, Warangal in 1982 and Ph.D from JNTU, Hyderabad in 2001. He is presently working as Principal of Priyadarshini Institute of Technology, Tirupati. He presented many research papers in various national and international journals and conferences. His researches areas include are in Electrical Machines and Power Electronic Drives.